Maresin 1 Protects the Liver Against Ischemia/Reperfusion Injury via the ALXR/Akt Signaling Pathway

Da Tang
Central South University Third Xiangya Hospital https://orcid.org/0000-0001-7178-0962
Guang Fu
Central South University Third Xiangya Hospital
Wenbo Li
Central South University second Xiangya Hospital
Ping Sun
Huazhong University of Science and Technology Tongji Medical College First Clinical College: Wuhan Union Hospital
Patricia A. Loughran
department of surgery univer,sity of pittsburgh
Meihong Deng
ohio state university medical school
Melanie J. Scott
University of Pittsburgh Department of Surgery
Timothy R. Billiar (billiartr@upmc.edu)
University of Pittsburgh https://orcid.org/0000-0002-2949-0811

Research article

Keywords: lipid mediators, hepatic ischemia/reperfusion, hepatocytes, inflammation, oxidative stress, apoptosis

Posted Date: November 11th, 2020

DOI: https://doi.org/10.21203/rs.3.rs-104054/v1

Version of Record: A version of this preprint was published on February 25th, 2021. See the published version at https://doi.org/10.1186/s10020-021-00280-9.

Abstract

Background

Hepatic ischemia/reperfusion (I/R) injury can be a major complication following liver surgery contributing to post-operative liver dysfunction. Maresin 1 (MaR1), a pro-resolving lipid mediator, has been shown to suppress I/R injury. However, the mechanisms that account for the protective effects of MaR1 in I/R injury remain unknown.

Methods

WT (C57BL/6) mice were subjected to partial hepatic warm ischemia for 60mins followed by reperfusion. Mice were treated with MaR1 (5-20ng/mouse), Boc2 (Lipoxin A4 receptor antagonist), LY294002 (Akt inhibitor) or corresponding controls just prior to liver I/R or at the beginning of reperfusion. Blood and liver samples were collected at 6h post-reperfusion. Serum aminotransferase, histopathologic changes, inflammatory cytokines, and oxidative stress were analyzed to evaluate liver injury. Signaling pathways were also investigated *in vitro* using primary mouse hepatocyte (HC) cultures to identify underlying mechanisms for MaR1 in liver I/R injury.

Results

MaR1 treatment significantly reduced ALT and AST levels, diminished necrotic areas, suppressed inflammatory responses, attenuated oxidative stress and decreased hepatocyte apoptosis in liver after I/R. Akt signaling was significantly increased in the MaR1-treated liver I/R group compared with controls. The protective effect of MaR1 was abrogated by pretreatment with Boc2, which together with MaR1-induced Akt activation. MaR1-mediated liver protection was reversed by inhibition of Akt.

Conclusions

MaR1 protects the liver against hepatic I/R injury via an ALXR/Akt signaling pathway. MaR1 may represent a novel therapeutic to mitigate the detrimental effects of I/R-induced liver injury.

Background

Liver ischemia-reperfusion (I/R) injury is a crucial contributor to liver damage and dysfunction after liver transplantation, partial hepatectomy, and hemorrhagic shock (Chen et al. 2020). Although great efforts have been made to explore therapeutic strategies to alleviate acute liver I/R injury, no pharmacologic intervention has been documented to be effective in preventing or treating this condition in clinical practice (van Golen et al. 2013). Therefore, more exploration into the potential mechanism and preventive strategies for hepatic I/R injury is urgently needed.

The pathophysiological process of liver I/R injury includes cell damage directly induced by ischemia, and subsequent severe hepatocyte damage caused by reperfusion-related inflammation (Guo et al. 2020,

(Zhang et al. 2018). During ischemia, hepatocytes are subjected to metabolic disturbance, which can directly initiate cell death. During reperfusion, the generation of reactive oxygen species (ROS) disturbs cellular redox status, which further contributes to cellular injury (Malhi et al. 2008). In response to oxidative stress, the recruitment and activation of Kupffer cells (KCs), monocytes and neutrophils produce damage-associated immune responses that can lead to hepatocyte apoptosis (Lentsch et al. 2000). Based on these observations, targeting the inflammatory response, apoptosis, and oxidative stress are promising approaches for ameliorating I/R related liver injury.

The n-3 polyunsaturated fatty acids (PUFAs), including eicosapentaenoic acid (EPA), arachidonic acid (AA), and docosahexaenoic acid (DHA), are dietary components and play important roles in many physiological processes (Chiang et al. 2019). A recent study emphasizes that endogenous n-3 PUFA-derived specialized pro-resolving mediators (SPMs), including maresins, lipoxins, protectins and resolvins, have potential anti-oxidative and anti-inflammatory properties (Serhan 2014). Maresins are biosynthetic derivatives of DHA synthesized in macrophages (Serhan et al. 2009). Recently, a number of studies have revealed that MaR1 exerts powerful anti-inflammatory and pro-resolving effects in several disease models by promoting the resolution of inflammation through reduced neutrophil infiltration and improved macrophage phagocytic activity without causing immunosuppression (Han et al. 2019, (Gong et al. 2015, (Buckley et al. 2014). Furthermore, studies also show that MaR1 has protective effects on I/R injury in several organs including the liver in a rat model (Soto et al. 2020). However, the mechanisms of the protective effects of MaR1 in hepatic I/R injury have not been established.

The aim of the current study was to examine the effect of MaR1 on hepatic damage in a mouse model of liver I/R and to define the mechanisms by which MaR1 reduces hepatocellular death during hepatic I/R injury. Our investigations highlight an unrecognized role for the ALXR (lipoxin A4 receptor) /Akt signaling pathway in MaR1-mediated antioxidant defenses during hepatic I/R injury.

Materials And Methods

Animals.

Male C57BL/6 wild-type (WT) were purchased from Jackson Laboratory and were bred at our animal facility. All experimental mice weighing 25–28 g used in this study were male and 8–12 weeks old. Animal protocols were approved by the Animal Care and Use Committee of the University of Pittsburgh and the experiments were performed in strict adherence to the NIH Guidelines for the Use of Laboratory Animals.

Reagents.

Western blot antibodies were purchased from Cell Signaling Technology and Novus Biologicals; LY294002 (# L9908) was obtained from Sigma-Aldrich. Mouse cytokine ELISA Kits were purchased from

R&D Systems. MaR1, MDA assay kit, and GPX activity assay kit were purchased from Cayman Chemical. Boc2 was obtained from Phoenix Pharmaceuticals, Inc.

Liver I/R model.

A nonlethal segmental (70%) hepatic warm ischemia-reperfusion model was used as previously described (Tsung et al. 2005). Briefly, the blood supply of the left and median liver lobes was interrupted with a microvascular clamp for 1 h and reperfusion was initiated by removing clamps. The temperature of the mice during the period of ischemia was maintained at 33 °C using an incubator chamber. Sham-operated mice underwent the same surgical procedure without vasculature occlusion. Serum and liver samples of mice were collected 6 h after reperfusion. MaR1 (5–20 ng/mouse; diluted with PBS) or PBS (control) was injected via tail vein at the beginning of reperfusion. Boc2 (50 mg/kg) or vehicle control was administrated into peritoneum 1 h before the surgical procedures. LY294002 (0.5 mg/kg, i.p.) was injected 30 min before I/R surgery.

Isolation, culture, and treatment of hepatocytes and nonparenchymal cells.

Hepatocytes (HCs) were isolated from mice as previously described (Lei et al. 2018). Briefly, HCs were separated from nonparenchymal cells (NPCs) through two cycles of differential centrifugation and further purified with a 30% Percoll gradient. HC purity exceeded 99% and HC cell viability was more than 95%. NPCs were isolated and purified without HCs as described (Yi et al. 2020). For HC&NPC co-culture, freshly isolated mouse HCs were seeded in collagen-coated 24 well plates at 1.5×10^5 cells/well in Williams' E medium and incubated for 2–4 h. Then, HCs were washed with PBS and overlaid with NPCs (7.5×10^5 cells/well) and incubated together. For experiments involving hypoxia, the cells were placed into a modular incubator chamber, which was equilibrated with the anoxic gas mixture (94% N_2, 5% CO_2, and 1% O_2.). For experiments using MaR1, 10 nM, 30 nM or 100 nM was added to the cell media 30 min prior to treatment with hypoxia. After incubating under hypoxia for 10 h, primary cells were incubated under normoxic conditions (air/5% CO2) for another 10 h. The cells and supernatants were collected for further analysis.

Liver damage assessment.

To assess the cellular injury and hepatic function following liver I/R injury, serum alanine aminotransferase (sALT) and serum aspartate transaminase (sAST) were evaluated using DRI-CHEM 4000 Chemistry Analyzer System (Heska). The percent necrotic area in the ischemic lobes was determined by the random assessment of each H&E stained histological section using Image J software.

Liver sections were scored using Suzuki methodology for characterizing I/R induced liver damage (Suzuki et al. 1993).

Cytokine quantification.

Serum IL-6, IL-10 and IL-1β levels in the mice were detected by ELISA kits (R&D Systems) according to the manufacturer's instructions.

Measurement of malondialdehyde (MDA) and Glutathione peroxidase (GPX) levels.

Frozen liver samples were weighed and homogenized. After centrifugation, the supernatants were collected for further experiments. MDA level and GPX activity were estimated by their respective commercial assay kits (Cayman Chemical) according to the manufacturer's protocol.

Immunofluorescent staining.

Liver samples were prepared as described. Briefly, ischemic liver lobes were cryoprotected in 2% paraformaldehyde for 2 h and then 30% sucrose for another 24 h. After that, the liver samples were cut into 6μm sections and placed onto slides. Immunofluorescent staining was begun by rehydrating the slides with PBS. Then, the liver sections were blocked with PBS + 20% normal goat serum (NGS) for 45 min. All samples were incubated with the specific primary antibody for lymphocyte antigen 6G [Ly6G] (1:100, BD Biosciences, catalog 560599) for 60 min. The sections were washed with 0.5% BSA three times and then the secondary antibody was incubated for another 60 min. Finally, all groups were stained for F-actin and nuclear staining. Cell death was evaluated by incubating with In Situ Cell Death Detection TMR Red (1:1000 Roche no. 12156792910) according to the manufacturer's protocol. Images were taken by a Nikon A1 confocal microscope. Quantification was performed using NIS Elements (Nikon).

Immunoblotting.

Western blot analysis was performed using whole-cell lysates from either ischemic liver lobes or HCs as previously described (Huang et al. 2014). The membranes were blocked in 5% milk for 1–2 h and then incubated overnight using the following primary antibodies (Cell Signaling Technology): β-actin, ERK, phospho-ERK, JNK, phospho-JNK, p38, phospho-p38, Akt, phospho-Akt, Bcl-2-associated X protein (Bax), B-cell lymphoma 2 (Bcl2), cleaved-caspase3, and ALXR (Novus Biologicals). Membranes were washed in TBST for 10 min, incubated with HRP-conjugated secondary antibody for 60 min, and then washed for 30 min in TBST before being detected by chemiluminescence (Thermo Fisher Scientific).

Lactate dehydrogenase assay.

Lytic cell death in HCs subjected to H/R treatment was evaluated by measurement of lactate dehydrogenase (LDH) released into the cell medium. After centrifugation, 50□L of the medium was transferred to a 96-well plate, and the levels of LDH were analyzed using Pierce LDH Cytotoxicity Assay Kit (Thermo Scientific) according to the manufacturer's instructions.

Cell viability assay.

To evaluate the effects of MaR1 on cell viability, primary HCs (2×10^4 cells/mL) and NPCs (1×10^5 cells/mL) were seeded into 96-well plates in a volume of 100uL per well. After treatment with MaR1 for 24 h, the CCK-8 kit was used to measure the cell viability.

Statistics.

Data analysis was performed using GraphPad Prism software. Results are shown as the mean±SEM. Group comparisons were analyzed using Student's *t*-test or ANOVA. Differences were considered significant at $P<0.05$.

Results

Maresin1 alleviates liver I/R injury in a dose-dependent manner

First, to determine whether MaR1 could prevent liver I/R injury in mice, WT mice were given i.v. injections of PBS or different doses of MaR1 at the beginning of reperfusion. Liver injury was examined at 6 h post-reperfusion. Treatment with 5 ng/mouse MaR1 had no effect on serum ALT (sALT) and serum AST (sAST) levels, however, doses of 10 ng/mouse and 20 ng/mouse MaR1 significantly reduced I/R-induced sALT and sAST levels (Fig. 1A, B), showing that MaR1-mediated protection from I/R induced liver injury was dose-dependent. The optimal effect of MaR1 was observed at 20 ng/mouse. Hence, 20 ng/mouse MaR1 was chosen for our subsequent experiments. Severe hepatocellular necrosis was present in liver sections from mice that were treated with PBS, whereas necrotic areas were significantly reduced in liver samples from MaR1-treated mice (20 ng/mouse) (Fig. 1C). The extent of necrosis and Suzuki's histological scores confirmed by H&E staining of liver tissues were consistent with ALT and AST levels (Fig. 1D, E). Together, these data indicate that the administration of MaR1 confers protection against hepatic I/R injury in a mouse model.

MaR1 protects hepatocytes from cell death bothin vivoandin vitro

Hepatocellular apoptosis is prominent in hepatic I/R injury (Malhi et al. 2006). To further investigate the protective role of MaR1 in the liver following I/R insult, TMR staining, a method to detect single-and double-stranded DNA breaks, was employed to assess the extent of cell death. There were fewer TMR-positive cells in the livers of the MaR1-treated I/R group than in those of PBS-treated mice (Fig. 2A, B). In addition, several pro-apoptotic and anti-apoptotic factors were evaluated by Western blotting. As expected, lower cleaved-caspase 3 protein levels were observed in livers from MaR1-treated mice compared with PBS-treated mice (Fig. 2C), indicating MaR1 protected liver cells from apoptosis after I/R. However, Bcl-2 and Bax levels were comparable between the two groups (Fig. 2C). To further assess the role of MaR1 *in vitro*, cultured primary hepatocytes (HCs) and nonparenchymal cells (NPCs) were treated with increasing concentrations of MaR1, and a CCK-8 assay was used to evaluate the cell viability. MaR1 concentrations of less than 300 nM did not affect cell viability under normoxic conditions (Supplementary Fig. 1). Primary HCs and NPCs were isolated from WT mice and subjected to hypoxia (1% O_2) and reoxygenation (H/R; 10 h hypoxia/10 h reoxygenation) in the presence or absence of MaR1. Lytic cell death was assessed by LDH release into the medium. MaR1 (100 nM) dramatically suppressed LDH release in primary HCs cultured alone or with NPCs, whereas the protective effects of MaR1 were not observed in NPCs cultured alone (Fig. 2D). In line with the *in vivo* results, MaR1 also contributed to lower levels of hepatocyte apoptosis when compared with vehicle-treated hepatocytes after H/R, as demonstrated by lower cleaved-caspase 3 protein levels (Fig. 2E). Collectively, these findings suggest that MaR1 is capable of reducing oxidative stress-induced cell death in HCs independent of NPCs.

MaR1 suppresses inflammatory responses following liver I/R injury

Previous studies have demonstrated that pro-resolving lipid mediators such as maresins can protect tissues by suppressing damaging inflammation (Sun et al. 2017). Therefore, we examined the serum levels of inflammatory cytokines. Interestingly, we found that MaR1 attenuated systemic inflammation after liver I/R, as shown by significantly lower levels of both serum IL-6 and IL-1β compared to the control mice (Fig. 3A, B), whereas IL-10 levels were not significantly influenced by the treatment of MaR1 (Fig. 3C). Additionally, immunofluorescence staining revealed that numbers of LY6G-positive neutrophils were significantly reduced in livers of MaR1-treated mice after I/R insult (Fig. 3D, E). Among numerous signaling programs, the MAPK pathway has been well-recognized in regulating inflammatory response as well as cell survival following I/R injury (Sun et al. 2015). Western blotting revealed that only the expression of p-ERK, but not p-P38 or p-JNK, was suppressed in the MaR1-treated I/R group when compared with the control I/R group (Fig. 3F, G). These results show that MaR1 restrains both systemic and local inflammation in response to hepatic I/R insult *in vivo*, and the ERK pathway is suppressed by MaR1 in I/R injury.

MaR1 suppressed oxidative stress during liver I/R injury.

Oxidative stress is also a crucial culprit to hepatocellular damage following I/R injury. To further investigate the effects of MaR1 on oxidative stress induced by liver I/R, the liver levels of malondialdehyde (MDA), a product of lipid peroxidation, (Gu et al. 2018) were evaluated. MDA levels were elevated in the I/R-treated mice compared with those in the sham surgery (Fig. 4A). A reduction in MDA generation was detected in the MaR1-mediated I/R group as compared with the PBS-treated I/R groups (Fig. 4A). Concomitant to the decreased MDA levels, a significant increase in the activity of the antioxidant enzyme glutathione peroxidase (GPX) was observed in the livers of the MaR1-treated I/R group as compared with that found in the PBS-treated I/R groups (Fig. 4B). These findings reveal that MaR1 reduces I/R-induced oxidative stress potentially via a mechanism involving enhanced antioxidant enzyme activity (GPX) in the liver.

Inhibition of lipoxin A4 receptor (ALXR) abolishes the beneficial effects of MaR1 in I/R-induced liver damage.

Previous findings demonstrated that MaR1 exerts its function via interacting with lipoxin A4 receptor (ALXR) in CLP-induced sepsis, and the salutary effect of MaR1 could be blocked by Boc2, an ALXR antagonist (Gu et al. 2018). To get a better understanding of the underlying mechanisms, we also explored the role of ALXR on MaR1-mediated protective effects in liver I/R injury. First, by Western blotting analysis, an antibody against ALXR revealed that an immunoreactive band around 38 kDa was expressed in both HCs and NPCs under normoxic conditions (Fig. 5A). While sALT and sAST levels were significantly lower in MaR1-treated I/R mice, the administration of Boc2 with MaR1 significantly prevented the effect of MaR1 on sALT and sAST levels (Fig. 5B, C). Similarly, the beneficial impact of MaR1 on the morphologic changes of liver damage was reversed by Boc2 (Fig. 5D, E). In addition, the MaR1-mediated reduction in serum IL-6 levels and cleaved-casp3 levels induced by MaR1 in I/R injury were also abolished by the pretreatment of Boc2 (Fig. 5F, G). Collectively, these data demonstrate that MaR1 exerts a protective role in I/R-induced liver damage via an ALXR-dependent pathway.

MaR1-induced Akt activation in hepatic I/R injury is dependent on ALXR.

Previous studies showed that Akt signaling is activated following hepatic I/R injury and protects against cell death (Zhang et al. 2014). To further elucidate the regulatory mechanism by which MaR1 affects liver I/R injury, we next investigated the function of the Akt pathway on MaR1-mediated amelioration of liver I/R damage. Consistent with published studies, Akt signaling was activated in I/R-induced liver injury (Fig. 6A). MaR1-treated mice exhibited enhanced Akt activation at 6 h post-reperfusion compared with PBS-treated mice (Fig. 6A), and Boc2 treatment blocked MaR1-mediated activation of Akt (Fig. 6B). To further explore whether the Akt pathway is necessary for MaR1 to protect against hepatic I/R insult an Akt

inhibitor, LY294002, was injected just prior to liver I/R. Western blotting revealed that the Akt inhibitor diminished phosphorylated Akt levels in the liver tissues of PBS-treated and MaR1-treated mice at 6 h after I/R injury when compared with their corresponding control groups (Fig. 6C, D). Measurement of sALT and histological estimation of the liver sections demonstrated that Akt inhibitor treatment significantly accentuated liver damage in both PBS- and MaR1-treated mice (Fig. 6E-G). Most importantly, treatment with Akt inhibitor completely abrogated MaR1-mediated liver protection (Fig. 6E-G). Additionally, Akt inhibition led to a failure of MaR1 to suppress inflammatory responses (IL-6; Fig. 6H) or reduce apoptosis (cleaved-casp3; Fig. 6I). These *in vivo* results support the conclusion that MaR1 confers protection against liver I/R injury via the activation of an ALXR/Akt signaling pathway.

Discussion

Hepatic I/R can contribute to severe liver damage and is a major clinical problem during liver surgical procedures. Studies of the pathophysiology and underlying mechanisms of liver I/R injury have yielded a number of potential therapeutic alternatives (Gracia-Sancho et al. 2015). However, effective therapeutics in rodent models are limited, and no pharmaceutical therapies specifically target I/R-induced liver injury have been approved for human use. Thus, preventing and attenuating hepatic I/R injury is an unmet clinical need. In this study, we confirm that MaR1 protects against deterioration of liver function in a mouse liver I/R model. The mechanism of hepatoprotection of MaR1 involved anti-inflammatory, anti-apoptosis and anti-oxidative effects during hepatic I/R injury. We show here that MaR1 acts via a known signaling partner, ALXR, to enhance activation of Akt with downstream effects on inflammatory responses and apoptosis resulting in alleviation of I/R-mediated liver damage (Fig. 7).

Previous studies investigating *in vivo* effects of MaR1 in rats used doses of 4 ng/g body weight given intraperitoneally 1 h prior to liver I/R (Soto et al. 2020). However, we investigated the effects of different doses of MaR1 given at the beginning of reperfusion via the tail vein. We found that a dose of MaR1 of 20 ng/mouse, effective to suppress I/R injury in mice. Thus, the use of MaR1 at the time of I/R could be therapeutically useful.

Numerous studies have provided strong evidence that inflammation-driven by reperfusion-mediated responses is the major contributor to liver damage in I/R injury (Jiménez-Castro et al. 2019), (van Golen et al. 2012). Increased levels of circulating inflammatory cytokines are associated with greater liver I/R injury (Liu et al. 2019). Therefore, recent efforts for therapeutic strategies have focused on the direct suppression of inflammation at the reperfusion stage (Datta et al. 2013, (Selzner et al. 2003). MaR1 has a series of pro-resolving actions including improved macrophage phagocytosis, diminished neutrophil infiltration and reduced pro-inflammatory cytokine release (Serhan et al. 2009, (Buckley et al. 2014). Consistent with these previous investigations, we found that treatment with MaR1 significantly decreased the serum IL-1β and IL-6 levels after hepatic I/R injury. Moreover, there were reduced Ly6G-positive inflammatory cells in MaR1-treated mouse livers. Similarly, we demonstrated that MaR1 negatively regulates ERK signaling, a pivotal component regulating inflammation and cell death, both *in vivo* and *in vitro* following liver I/R injury. Taken together, these results demonstrate that MaR1 effectively modulates

inflammatory responses after liver I/R. We speculate that this may occur, in part, through the suppression of cellular death.

In addition to inflammation, recent evidence indicated that apoptosis is another essential contributor to hepatic I/R injury (Guo et al. 2020). Apoptosis can also be enhanced by reperfusion-induced inflammatory responses (Jassem et al. 2019). We confirmed that MaR1-treated mice exhibited decreased hepatocyte apoptosis compared with controls after liver I/R. However, this is contradictory to previous findings in a rat liver I/R model, where protein expression of cleaved caspase-3 was dramatically increased with MaR1 treatment (Soto et al. 2020). The reason for the contradictory results is unclear and may be related to species differences, time of treatment with MaR1, or potential adverse/toxic effects of MaR1 in the previously-published study.

In this study, we are the first to demonstrate that the protective role of MaR1 on hepatic I/R injury is independent of NPCs, which suggests that MaR1 has a direct effect on HCs. Hepatic I/R injury is a complicated pathological state, in which oxidative stress also exerts a critical role (Yi et al. 2020). During the reperfusion period, HCs, neutrophils and macrophages can produce ROS, which can trigger the activation of the inflammatory immune responses (Jaeschke 2011). Furthermore, the excess generation of ROS, leading to protein and DNA damage through lipid peroxidation, is regarded as a major cause of oxidative damage to cellular membranes during I/R injury (Rani et al. 2016). In our study, the level of tissue MDA, a main product of lipid peroxidation, was markedly decreased in the MaR1-treated mouse livers following hepatic I/R insult. The eradication of reactive free radicals is dependent on many different antioxidant enzymes, such as superoxide dismutase (SOD), glutathione peroxidase (GPX) and catalase (CAT), which keep the balance between antioxidative effects and oxidative stress responses (Sun et al. 2017). Loss of antioxidant enzymes causes accumulation of free radicals, which further exacerbates I/R-induced injury (Han et al. 2016). Our study reveals a novel effect of MaR1 on the formation of MDA potentially via increased antioxidative enzyme (e.g. GPX) activity during hepatic I/R injury. Thus, it is reasonable to assume that the beneficial effects of MaR1 on liver I/R injury are, at least, partly due to maintenance of the balance between antioxidative and oxidative stresses.

It has been widely accepted that the SPMs, such as MaR1, exert anti-inflammatory actions through direct binding to their corresponding G protein-coupled receptors (GPCRs) (Serhan 2010). However, due to the complicated cellular context, each receptor is capable of interacting with more than one SPM. Previous studies suggested that MaR1 could interact with ALXR (lipoxin A4 receptor) in CLP-induced sepsis in mice to induce protection (Gu et al. 2018). Other studies revealed that resolving E1, another SPM, could induce the generation of endogenous lipoxin A4 in the lung, which was similarly protective (Haworth et al. 2008). In the present study, we confirmed a role for ALXR in mediating the protective effects of MaR1 in liver I/R, although this could be via acting directly at ALXR, or induction of lipoxin A4 production via another MaR1-induced signaling pathway. Further study will be needed to determine which pathway dominates.

Akt is a downstream effector of PI3K signaling shown to modulate multiple cellular effects (Martin et al. 2005). Akt signaling is a known regulator of liver I/R injury (Li et al. 2019), and there is increasing evidence that Akt signaling initiates cell survival through inhibition of apoptosis and improving cell viability (Tsuruta et al. 2002). Our studies showed that MaR1 increases Akt activation/phosphorylation after I/R injury and this was dependent on ALXR signaling. More importantly, Akt upregulation and activation were critical for MaR1-mediated hepatoprotection in liver I/R injury, which is also in line with published studies (Sun et al. 2015, (Izuishi et al. 2006).

In conclusion, our present study provides evidence that MaR1 exerts a protective role in I/R-induced injury by reducing the inflammatory response and alleviating hepatocyte apoptosis via ALXR/Akt signaling. These observations broaden our deeper understanding of the direct regulatory role of MaR1 on hepatic I/R insult. Significantly, MaR1 is an endogenous chemical mediator with few identified side effects, suggesting that MaR1 has the potential to be used therapeutically in a wide range of human diseases induced by I/R injury.

Abbreviations

I/R, ischemia/reperfusion; H/R, hypoxia/reoxygenation; MaR1, Maresin 1; ALT, alanine aminotransferase; AST, aspartate aminotransferase; IL-1β, interleukin-1β; IL-6, interleukin 6; IL-10, interleukin 10; LDH, lactate dehydrogenase; MAPK, mitogen-activated protein kinase; JNK, c-Jun-N-terminal kinase; ERK, extracellular signal-regulated kinase; ALXR, Lipoxin A4 receptor; MDA, malondialdehyde; SOD, superoxide dismutase; GPX, glutathione peroxidase; CAT, catalase; HC, hepatocyte; NPC, nonparenchymal cell; SPM, specialized pro-resolving mediator; CLP, cecal ligation and puncture; Bax, Bcl-2-associated X protein; Bcl2, B-cell lymphoma 2; LDH, lactate dehydrogenase.

Declarations

Ethics approval and consent to participate

The current study was performed in the Department of Surgery, University of Pittsburgh, with the institutional ethical committee approval. Animal protocols were approved by the Animal Care and Use Committee of the University of Pittsburgh and the experiments were performed in strict adherence to the NIH Guidelines for the Use of Laboratory Animals.

Consent for publication

Not applicable.

Availability of data and materials

The datasets used and/or analyzed during the current study are available from the corresponding author on reasonable request.

Competing interests

The authors declare that they have no competing interests.

Funding

This study was supported by grant awards from NIH to T.R.B (R35GM127027) and M.J.S (R01GM102146).

Author's Contributions

DT and TRB conceived the project and designed experiments and wrote the manuscript; DT designed and performed the experiments and analyzed the data; MD and MJS. supervised the study and wrote the manuscript; PAL collected the images and analyzed the data. GF performed the mouse experiments and participated in data collection; WL and PS analyzed the data and put the figures together. All authors read and approved the final manuscript.

Acknowledgments

We thank Hong Liao for outstanding technical assistance.

References

1. Chen SY, Zhang HP, Li J, Shi JH, Tang HW, Zhang Y, et al. Tripartite motif-containing 27 attenuates liver ischemia/reperfusion injury by suppressing TAK1 via TAB2/3 degradation. Hepatology (Baltimore, Md.). 2020.
2. van Golen RF, Reiniers MJ, Olthof PB, van Gulik TM, Heger M. Sterile inflammation in hepatic ischemia/reperfusion injury: present concepts and potential therapeutics. Journal of gastroenterology and hepatology. 2013;28(3):394-400.
3. Guo WZ, Fang HB, Cao SL, Chen SY, Li J, Shi JH, et al. Six-Transmembrane Epithelial Antigen of the Prostate 3 Deficiency in Hepatocytes Protects the Liver Against Ischemia-Reperfusion Injury by Suppressing Transforming Growth Factor-β-Activated Kinase 1. Hepatology (Baltimore, Md.). 2020;71(3):1037-54.
4. Zhang XJ, Cheng X, Yan ZZ, Fang J, Wang X, Wang W, et al. An ALOX12-12-HETE-GPR31 signaling axis is a key mediator of hepatic ischemia-reperfusion injury. Nature medicine. 2018;24(1):73-83.

5. Malhi H, Gores GJ. Cellular and molecular mechanisms of liver injury. Gastroenterology. 2008;134(6):1641-54.
6. Lentsch AB, Kato A, Yoshidome H, McMasters KM, Edwards MJ. Inflammatory mechanisms and therapeutic strategies for warm hepatic ischemia/reperfusion injury. Hepatology (Baltimore, Md.). 2000;32(2):169-73.
7. Chiang N, Libreros S, Norris PC, de la Rosa X, Serhan CN. Maresin 1 activates LGR6 receptor promoting phagocyte immunoresolvent functions. The Journal of clinical investigation. 2019;129(12):5294-311.
8. Serhan CN. Pro-resolving lipid mediators are leads for resolution physiology. Nature. 2014;510(7503):92-101.
9. Serhan CN, Yang R, Martinod K, Kasuga K, Pillai PS, Porter TF, et al. Maresins: novel macrophage mediators with potent antiinflammatory and proresolving actions. The Journal of experimental medicine. 2009;206(1):15-23.
10. Han YH, Shin KO, Kim JY, Khadka DB, Kim HJ, Lee YM, et al. A maresin 1/RORα/12-lipoxygenase autoregulatory circuit prevents inflammation and progression of nonalcoholic steatohepatitis. The Journal of clinical investigation. 2019;129(4):1684-98.
11. Gong J, Liu H, Wu J, Qi H, Wu ZY, Shu HQ, et al. MARESIN 1 PREVENTS LIPOPOLYSACCHARIDE-INDUCED NEUTROPHIL SURVIVAL AND ACCELERATES RESOLUTION OF ACUTE LUNG INJURY. Shock (Augusta, Ga.). 2015;44(4):371-80.
12. Buckley CD, Gilroy DW, Serhan CN. Proresolving lipid mediators and mechanisms in the resolution of acute inflammation. Immunity. 2014;40(3):315-27.
13. Soto G, Rodríguez MJ, Fuentealba R, Treuer AV, Castillo I, González DR, et al. Maresin 1, a Proresolving Lipid Mediator, Ameliorates Liver Ischemia-Reperfusion Injury and Stimulates Hepatocyte Proliferation in Sprague-Dawley Rats. International journal of molecular sciences. 2020;21(2).
14. Tsung A, Sahai R, Tanaka H, Nakao A, Fink MP, Lotze MT, et al. The nuclear factor HMGB1 mediates hepatic injury after murine liver ischemia-reperfusion. The Journal of experimental medicine. 2005;201(7):1135-43.
15. Lei Z, Deng M, Yi Z, Sun Q, Shapiro RA, Xu H, et al. cGAS-mediated autophagy protects the liver from ischemia-reperfusion injury independently of STING. American journal of physiology. Gastrointestinal and liver physiology. 2018;314(6):G655-g67.
16. Yi Z, Deng M, Scott MJ, Fu G, Loughran PA, Lei Z, et al. IRG1/Itaconate Activates Nrf2 in Hepatocytes to Protect Against Liver Ischemia-Reperfusion Injury. Hepatology (Baltimore, Md.). 2020.
17. Suzuki S, Toledo-Pereyra LH, Rodriguez FJ, Cejalvo D. Neutrophil infiltration as an important factor in liver ischemia and reperfusion injury. Modulating effects of FK506 and cyclosporine. Transplantation. 1993;55(6):1265-72.
18. Huang H, Nace GW, McDonald KA, Tai S, Klune JR, Rosborough BR, et al. Hepatocyte-specific high-mobility group box 1 deletion worsens the injury in liver ischemia/reperfusion: a role for intracellular

high-mobility group box 1 in cellular protection. Hepatology (Baltimore, Md.). 2014;59(5):1984-97.
19. Malhi H, Gores GJ, Lemasters JJ. Apoptosis and necrosis in the liver: a tale of two deaths? Hepatology (Baltimore, Md.). 2006;43(2 Suppl 1):S31-44.
20. Sun Q, Wu Y, Zhao F, Wang J. Maresin 1 Ameliorates Lung Ischemia/Reperfusion Injury by Suppressing Oxidative Stress via Activation of the Nrf-2-Mediated HO-1 Signaling Pathway. Oxidative medicine and cellular longevity. 2017;2017(9634803.
21. Sun P, Zhang P, Wang PX, Zhu LH, Du Y, Tian S, et al. Mindin deficiency protects the liver against ischemia/reperfusion injury. Journal of hepatology. 2015;63(5):1198-211.
22. Gu J, Luo L, Wang Q, Yan S, Lin J, Li D, et al. Maresin 1 attenuates mitochondrial dysfunction through the ALX/cAMP/ROS pathway in the cecal ligation and puncture mouse model and sepsis patients. Laboratory investigation; a journal of technical methods and pathology. 2018;98(6):715-33.
23. Zhang R, Zhang L, Manaenko A, Ye Z, Liu W, Sun X. Helium preconditioning protects mouse liver against ischemia and reperfusion injury through the PI3K/Akt pathway. Journal of hepatology. 2014;61(5):1048-55.
24. Gracia-Sancho J, Casillas-Ramírez A, Peralta C. Molecular pathways in protecting the liver from ischaemia/reperfusion injury: a 2015 update. Clinical science (London, England : 1979). 2015;129(4):345-62.
25. Jiménez-Castro MB, Cornide-Petronio ME, Gracia-Sancho J, Peralta C. Inflammasome-Mediated Inflammation in Liver Ischemia-Reperfusion Injury. Cells. 2019;8(10).
26. van Golen RF, van Gulik TM, Heger M. The sterile immune response during hepatic ischemia/reperfusion. Cytokine & growth factor reviews. 2012;23(3):69-84.
27. Liu Y, Lu T, Zhang C, Xu J, Xue Z, Busuttil RW, et al. Activation of YAP attenuates hepatic damage and fibrosis in liver ischemia-reperfusion injury. Journal of hepatology. 2019;71(4):719-30.
28. Datta G, Fuller BJ, Davidson BR. Molecular mechanisms of liver ischemia reperfusion injury: insights from transgenic knockout models. World journal of gastroenterology. 2013;19(11):1683-98.
29. Selzner N, Rudiger H, Graf R, Clavien PA. Protective strategies against ischemic injury of the liver. Gastroenterology. 2003;125(3):917-36.
30. Jassem W, Xystrakis E, Ghnewa YG, Yuksel M, Pop O, Martinez-Llordella M, et al. Normothermic Machine Perfusion (NMP) Inhibits Proinflammatory Responses in the Liver and Promotes Regeneration. Hepatology (Baltimore, Md.). 2019;70(2):682-95.
31. Jaeschke H. Reactive oxygen and mechanisms of inflammatory liver injury: Present concepts. Journal of gastroenterology and hepatology. 2011;26 Suppl 1(173-9.
32. Rani V, Deep G, Singh RK, Palle K, Yadav UC. Oxidative stress and metabolic disorders: Pathogenesis and therapeutic strategies. Life sciences. 2016;148(183-93.
33. Han X, Yao W, Liu Z, Li H, Zhang ZJ, Hei Z, et al. Lipoxin A4 Preconditioning Attenuates Intestinal Ischemia Reperfusion Injury through Keap1/Nrf2 Pathway in a Lipoxin A4 Receptor Independent Manner. Oxidative medicine and cellular longevity. 2016;2016(9303606.

34. Serhan CN. Novel lipid mediators and resolution mechanisms in acute inflammation: to resolve or not? The American journal of pathology. 2010;177(4):1576-91.
35. Haworth O, Cernadas M, Yang R, Serhan CN, Levy BD. Resolvin E1 regulates interleukin 23, interferon-gamma and lipoxin A4 to promote the resolution of allergic airway inflammation. Nature immunology. 2008;9(8):873-9.
36. Martin M, Rehani K, Jope RS, Michalek SM. Toll-like receptor-mediated cytokine production is differentially regulated by glycogen synthase kinase 3. Nature immunology. 2005;6(8):777-84.
37. Li S, Yi Z, Deng M, Scott MJ, Yang C, Li W, et al. TSLP protects against liver I/R injury via activation of the PI3K/Akt pathway. JCI insight. 2019;4(22).
38. Tsuruta F, Masuyama N, Gotoh Y. The phosphatidylinositol 3-kinase (PI3K)-Akt pathway suppresses Bax translocation to mitochondria. The Journal of biological chemistry. 2002;277(16):14040-7.
39. Izuishi K, Tsung A, Hossain MA, Fujiwara M, Wakabayashi H, Masaki T, et al. Ischemic preconditioning of the murine liver protects through the Akt kinase pathway. Hepatology (Baltimore, Md.). 2006;44(3):573-80.

Figures

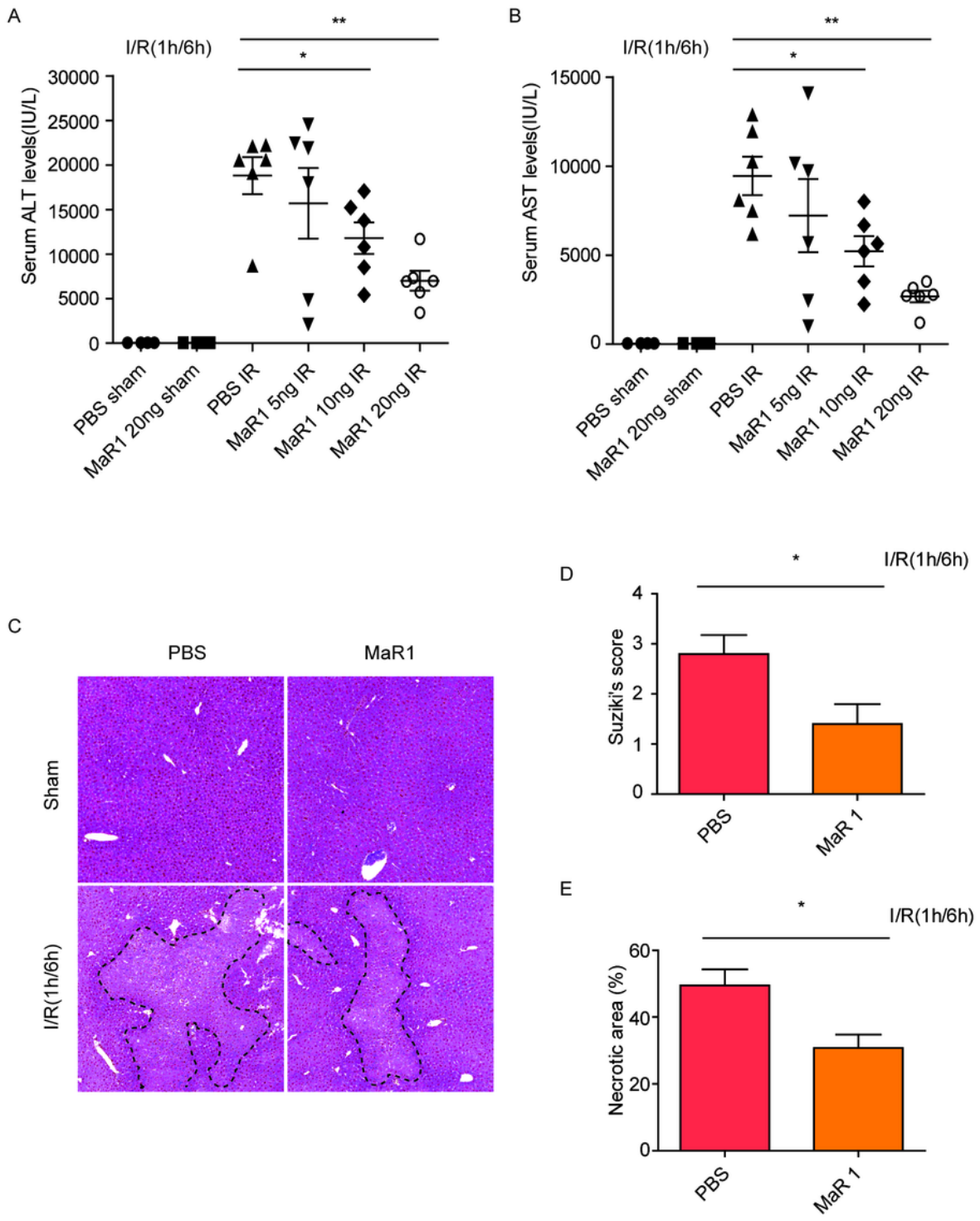

Figure 1

Low-dose MaR1 prevents liver I/R injury. WT mice were injected via tail vein with either PBS (control) or MaR1 at doses of 5ng, 10ng or 20ng/mouse at the beginning of reperfusion after 1h ischemia. Serum ALT (A) and AST (B) at 6h post-reperfusion. Plots show levels in individual mice (n=6/gp) with bars showing mean ± SEM. Liver H&E (original magnification ×20) from WT mice given PBS (control) or MaR1 (20ng/mouse) after 1h ischemia followed by 6h reperfusion or sham procedure (C). (D) Suzuki's

histological score of liver damage (n=5/gp); (E) Dotted lines indicate measured necrotic areas (quantified in bar graph (n=5/gp); Images are representative across all measured samples. Data are presented as mean ± SEM. *P <0.05, **P<0.01.

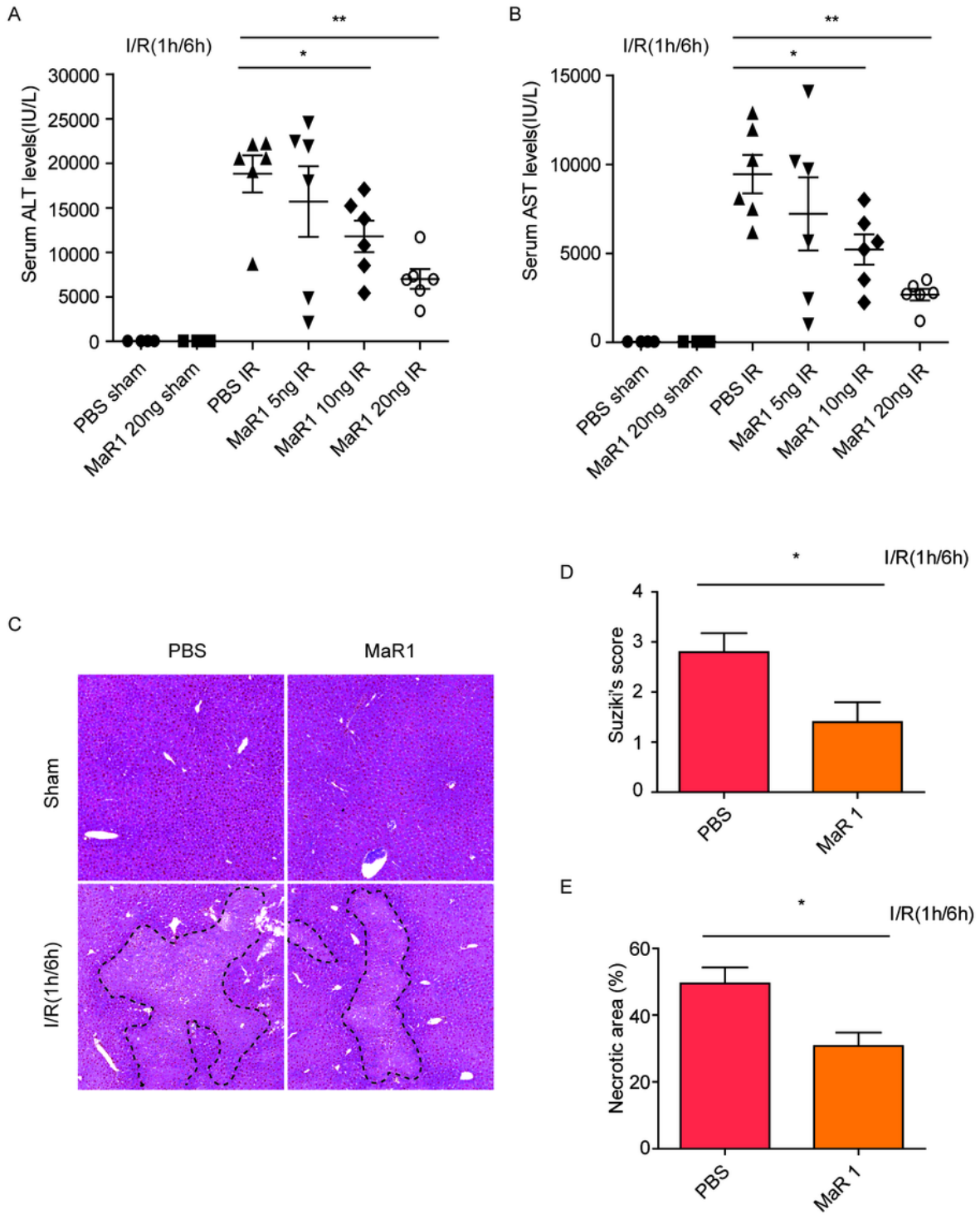

Figure 1

Low-dose MaR1 prevents liver I/R injury. WT mice were injected via tail vein with either PBS (control) or MaR1 at doses of 5ng, 10ng or 20ng/mouse at the beginning of reperfusion after 1h ischemia. Serum

ALT (A) and AST (B) at 6h post-reperfusion. Plots show levels in individual mice (n=6/gp) with bars showing mean ± SEM. Liver H&E (original magnification ×20) from WT mice given PBS (control) or MaR1 (20ng/mouse) after 1h ischemia followed by 6h reperfusion or sham procedure (C). (D) Suzuki's histological score of liver damage (n=5/gp); (E) Dotted lines indicate measured necrotic areas (quantified in bar graph (n=5/gp); Images are representative across all measured samples. Data are presented as mean ± SEM. *P <0.05, **P<0.01.

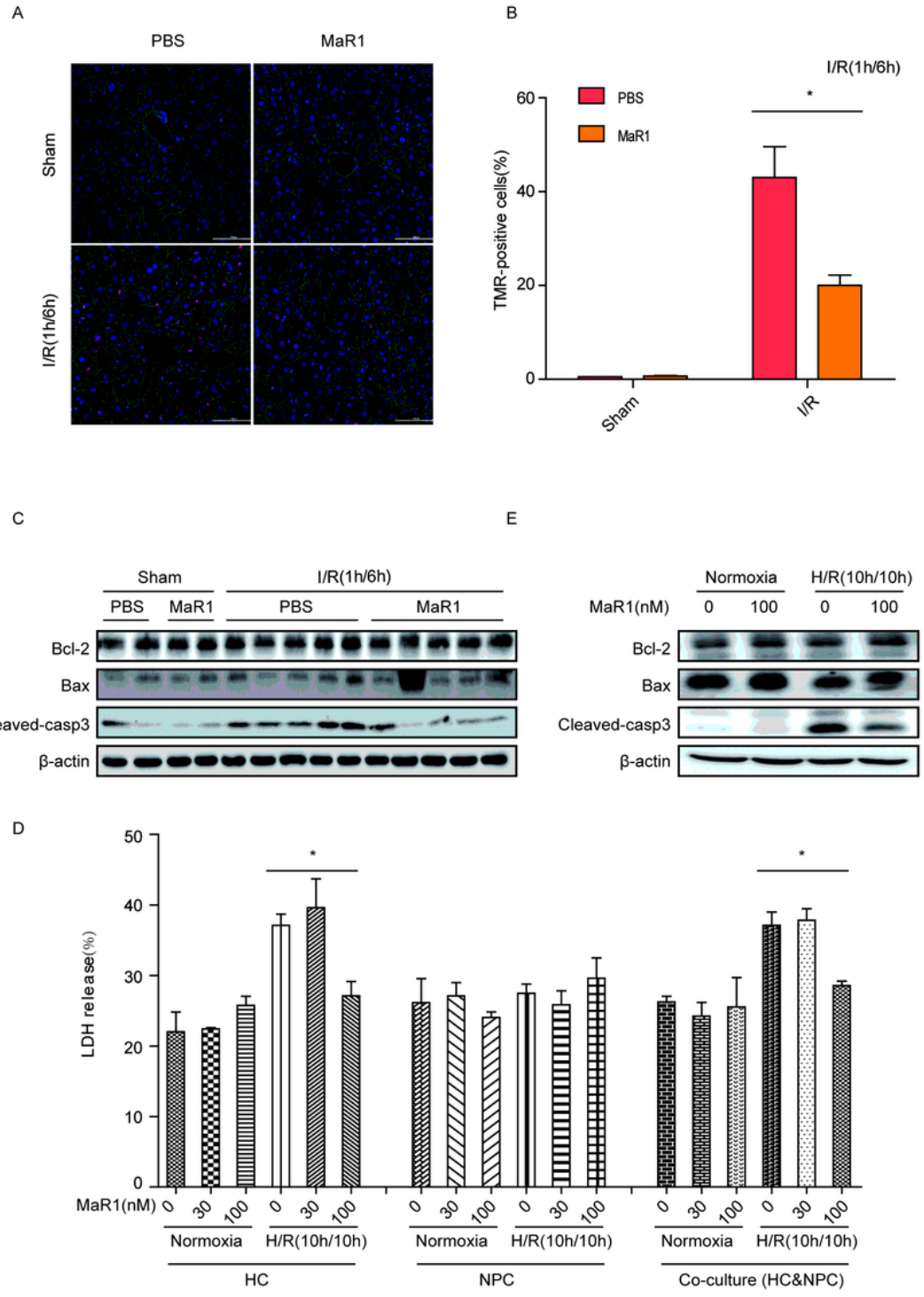

Figure 2

MaR1 reduces hepatocyte apoptosis during hepatic I/R injury. (A) Confocal images of TMR (red), nucleus (blue), and F-actin (green) in liver sections obtained from PBS or MaR1-treated mice subjected to sham surgery or 1h ischemia/6h reperfusion (scale bar = 100μm). (B) Percentage of TMR-positive cells per liver section (n=3 or 4/gp). (C) Western blot analysis of apoptosis markers (Bax, Bcl-2 and cleaved-caspase3) in liver tissues from PBS- and MaR1-treated mice that underwent sham operation or liver I/R insult (1h/6h). (D) LDH release in primary mouse HCs, NPCs, or HC/NPC co-cultures subjected to normoxia or 10h hypoxia (1%O2)/10h reoxia (H/R 10h/10h) without (0) or with pretreatment with 30 or 100nM MaR1. (E) Western blot analysis of Bcl-2, Bax and cleaved-caspase3 in primary mouse HCs treated with normoxia or H/R without (0) or with 100nM MaR1 given prior to H/R. Images representative of at least 3 separate experiments. All data are shown as mean ± SEM. *P <0.05.

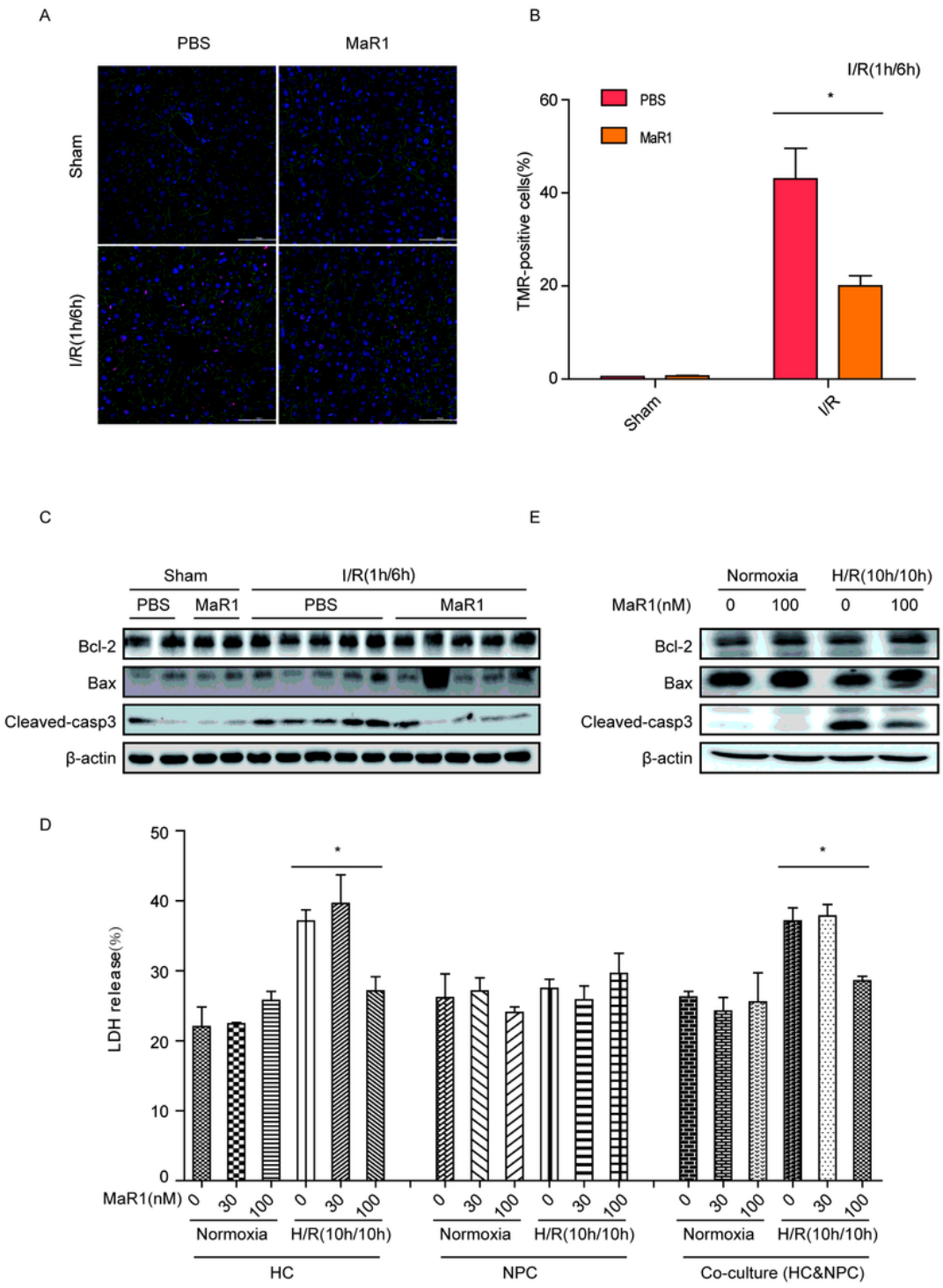

Figure 2

MaR1 reduces hepatocyte apoptosis during hepatic I/R injury. (A) Confocal images of TMR (red), nucleus (blue), and F-actin (green) in liver sections obtained from PBS or MaR1-treated mice subjected to sham surgery or 1h ischemia/6h reperfusion (scale bar = 100μm). (B) Percentage of TMR-positive cells per liver section (n=3 or 4/gp). (C) Western blot analysis of apoptosis markers (Bax, Bcl-2 and cleaved-caspase3) in liver tissues from PBS- and MaR1-treated mice that underwent sham operation or liver I/R insult

(1h/6h). (D) LDH release in primary mouse HCs, NPCs, or HC/NPC co-cultures subjected to normoxia or 10h hypoxia (1%O2)/10h reoxia (H/R 10h/10h) without (0) or with pretreatment with 30 or 100nM MaR1. (E) Western blot analysis of Bcl-2, Bax and cleaved-caspase3 in primary mouse HCs treated with normoxia or H/R without (0) or with 100nM MaR1 given prior to H/R. Images representative of at least 3 separate experiments. All data are shown as mean ± SEM. *P <0.05.

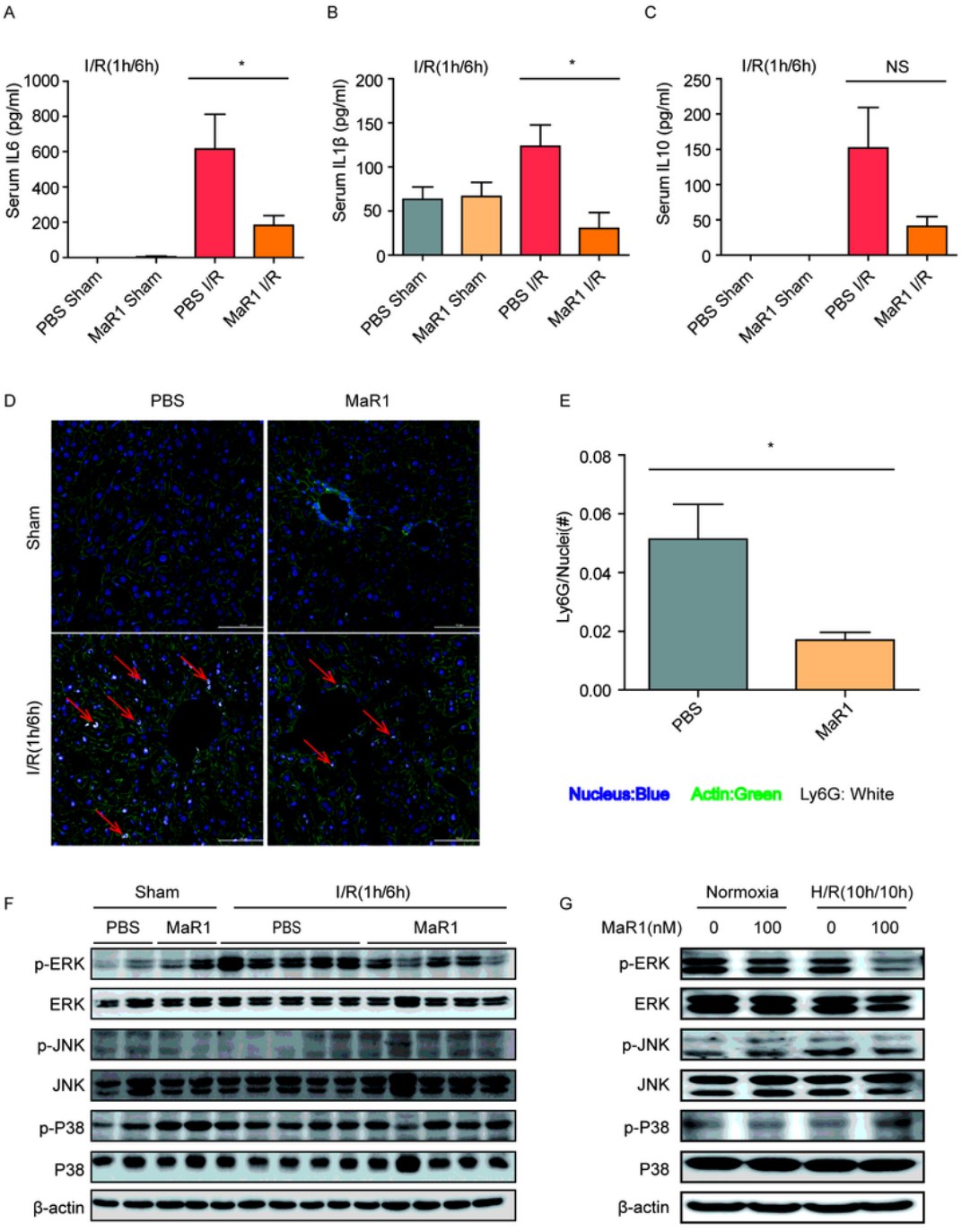

Figure 3

MaR1 inhibits inflammatory responses following hepatic I/R injury. Serum levels of cytokines IL-6 (A), IL-1β (B) and IL-10 (C) in WT mice after sham or I/R (1h/6h) treated with PBS or MaR1 (20ng/mouse) (n=6/gp). (D) Representative immunofluorescence staining of LY6G-positive inflammatory cells in ischemic lobes of mice in the indicated groups. Ly6G (white), nucleus (blue), and F-actin (green); (scale bar = 100μm; original magnification ×40). (E) Quantification of infiltrating Ly6G-positive neutrophils; n=3/gp. Western blot analysis of total and phosphorylated (p) ERK, JNK and p38 in liver after sham or I/R surgery (F) or primary mouse HC after H/R (G) with treatments as indicated. In vivo: n=5/gp; 20ng/mouse MaR1. In vitro: 100nM MaR1 given as a pretreatment. Images representative of at least 3 independent experiments. Results are expressed as mean ± SEM. *P < 0.05.

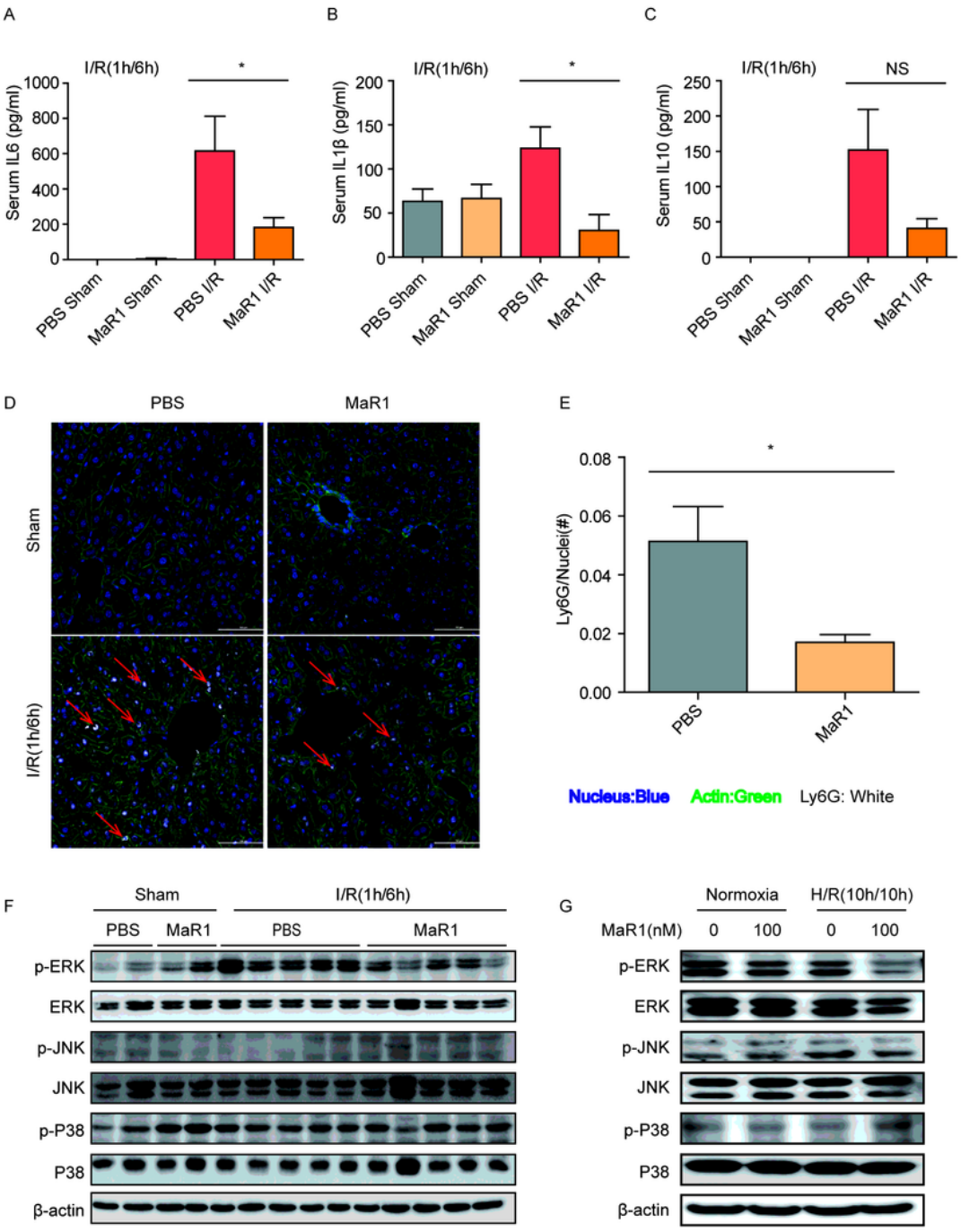

Figure 3

MaR1 inhibits inflammatory responses following hepatic I/R injury. Serum levels of cytokines IL-6 (A), IL-1β (B) and IL-10 (C) in WT mice after sham or I/R (1h/6h) treated with PBS or MaR1 (20ng/mouse) (n=6/gp). (D) Representative immunofluorescence staining of LY6G-positive inflammatory cells in ischemic lobes of mice in the indicated groups. Ly6G (white), nucleus (blue), and F-actin (green); (scale bar = 100μm; original magnification ×40). (E) Quantification of infiltrating Ly6G-positive neutrophils;

n=3/gp. Western blot analysis of total and phosphorylated (p) ERK, JNK and p38 in liver after sham or I/R surgery (F) or primary mouse HC after H/R (G) with treatments as indicated. In vivo: n=5/gp; 20ng/mouse MaR1. In vitro: 100nM MaR1 given as a pretreatment. Images representative of at least 3 independent experiments. Results are expressed as mean ± SEM. *P < 0.05.

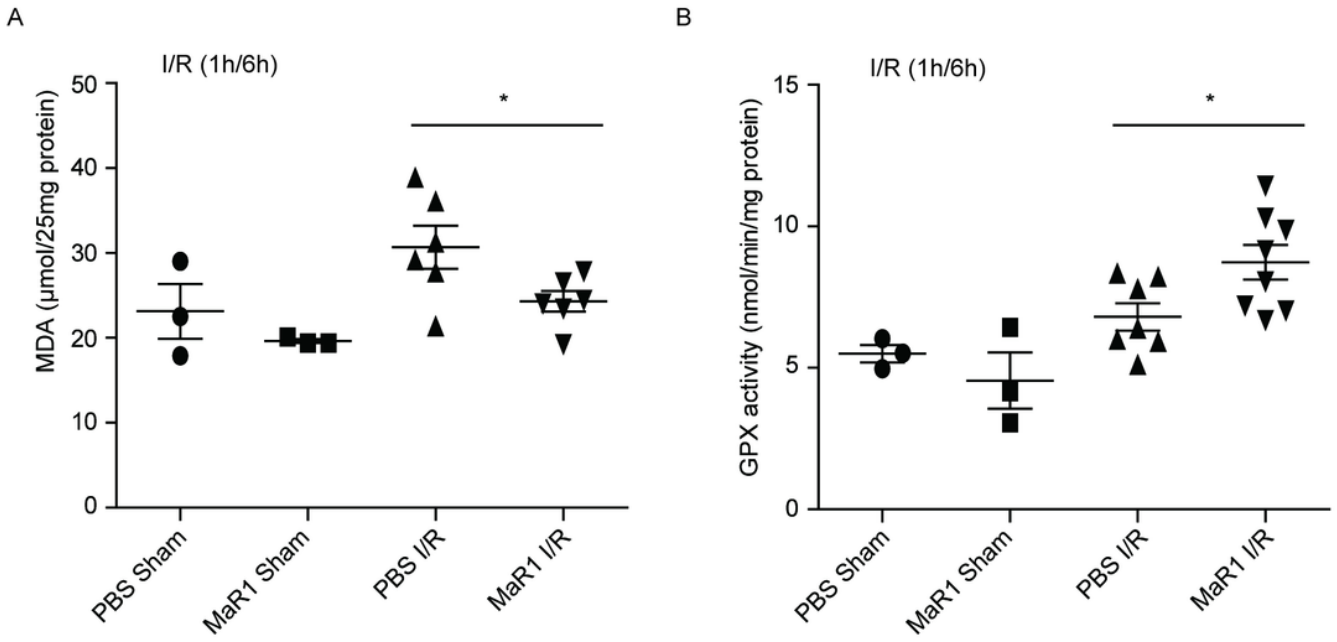

Figure 4

MaR1 suppresses oxidative stress in the liver after I/R injury. Quantitative analysis of concentration of malondialdehyde (MDA) (A) and glutathione peroxidase (GPX) (B) in liver tissues of WT mice after sham surgery or liver I/R (1h/6h) treated with PBS or MaR1 (20ng/mouse). Results are expressed as mean ± SEM. n=3 for sham groups; n= 6-8 for I/R group. *P < 0.05.

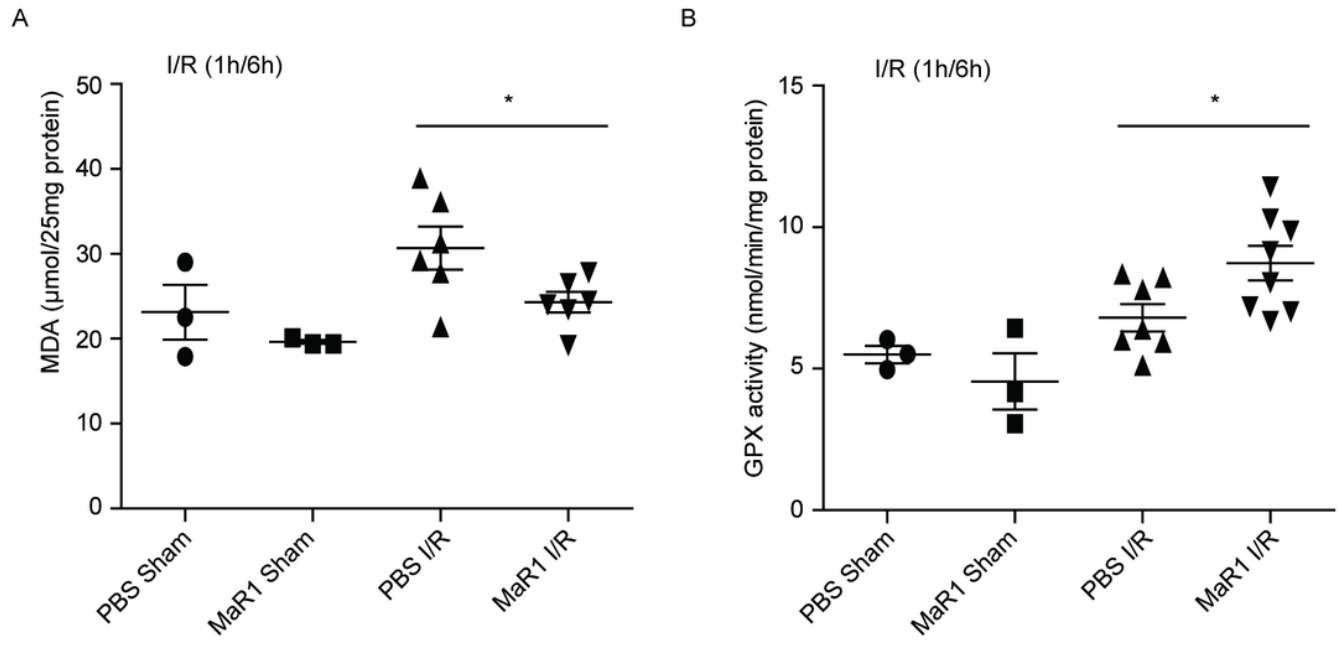

Figure 4

MaR1 suppresses oxidative stress in the liver after I/R injury. Quantitative analysis of concentration of malondialdehyde (MDA) (A) and glutathione peroxidase (GPX) (B) in liver tissues of WT mice after sham surgery or liver I/R (1h/6h) treated with PBS or MaR1 (20ng/mouse). Results are expressed as mean ± SEM. n=3 for sham groups; n= 6-8 for I/R group. *P < 0.05.

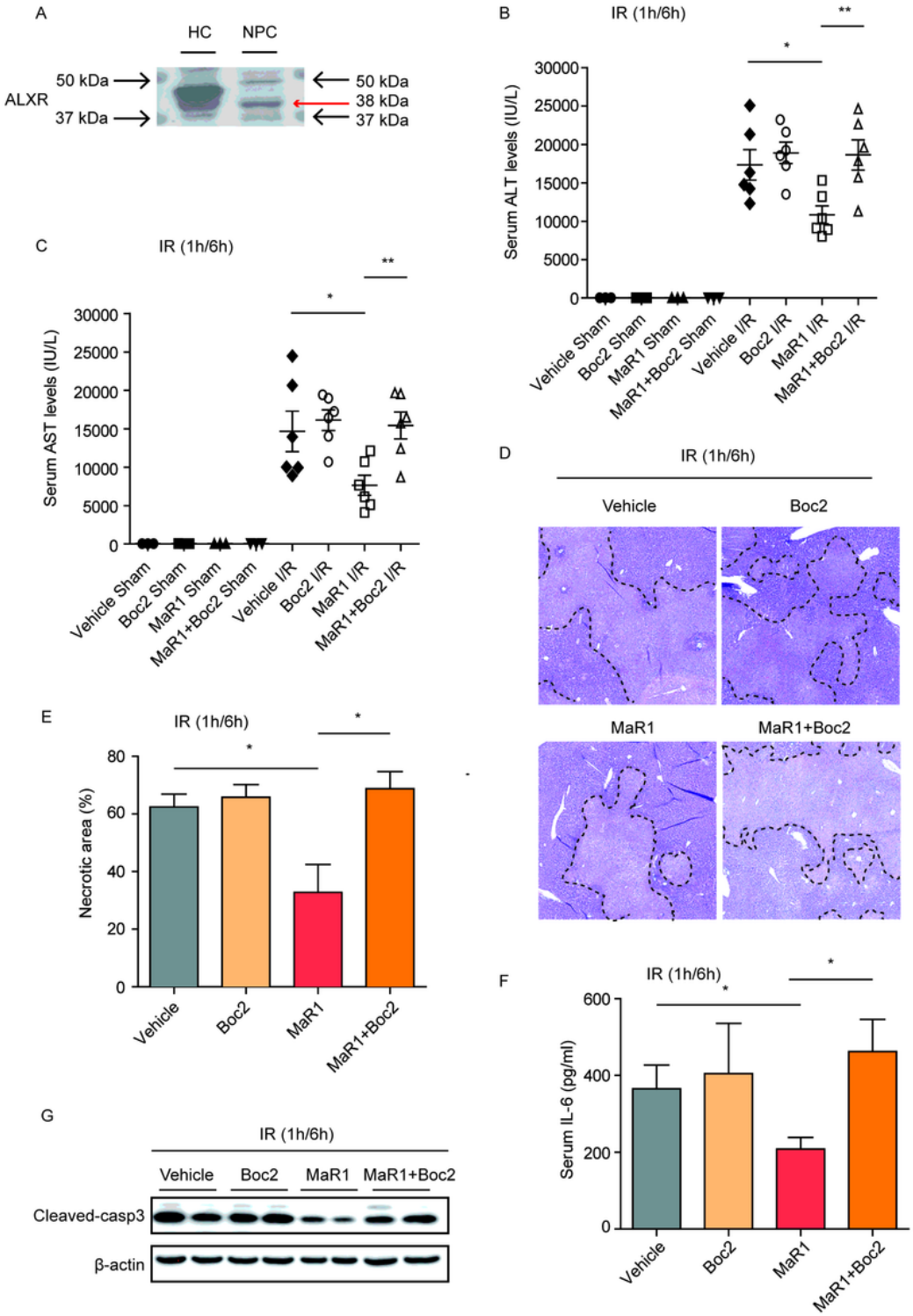

Figure 5

Inhibition of lipoxin A4 receptor (ALXR) abolishes the beneficial effects of MaR1 in I/R-induced liver damage. (A) Western blot of whole-cell lysates from primary mouse HC and NPC assessing protein expression of ALXR at the baseline. WT mice were treated with/without ALXR inhibitor (Boc2; 50mg/kg, i.p.) 1h prior to liver I/R with PBS or MaR1 (20ng/mouse, i.v.) (B, C) Serum ALT and AST levels in indicated groups after 6h reperfusion (n=3 in sham groups; n=6 in I/R groups). (D) Representative liver

H&E staining (original magnification ×20) from indicated groups. (E) Quantitation of liver necrotic areas, quantified in bar graph; n = 5 for each I/R group; (F) Serum IL-6 levels in indicated groups. (G) Western blot analysis of cleaved-caspase 3 in liver tissue from mice subjected to I/R insult in the indicated group. Data are presented as mean ± SEM. *P <0.05, **P<0.01.

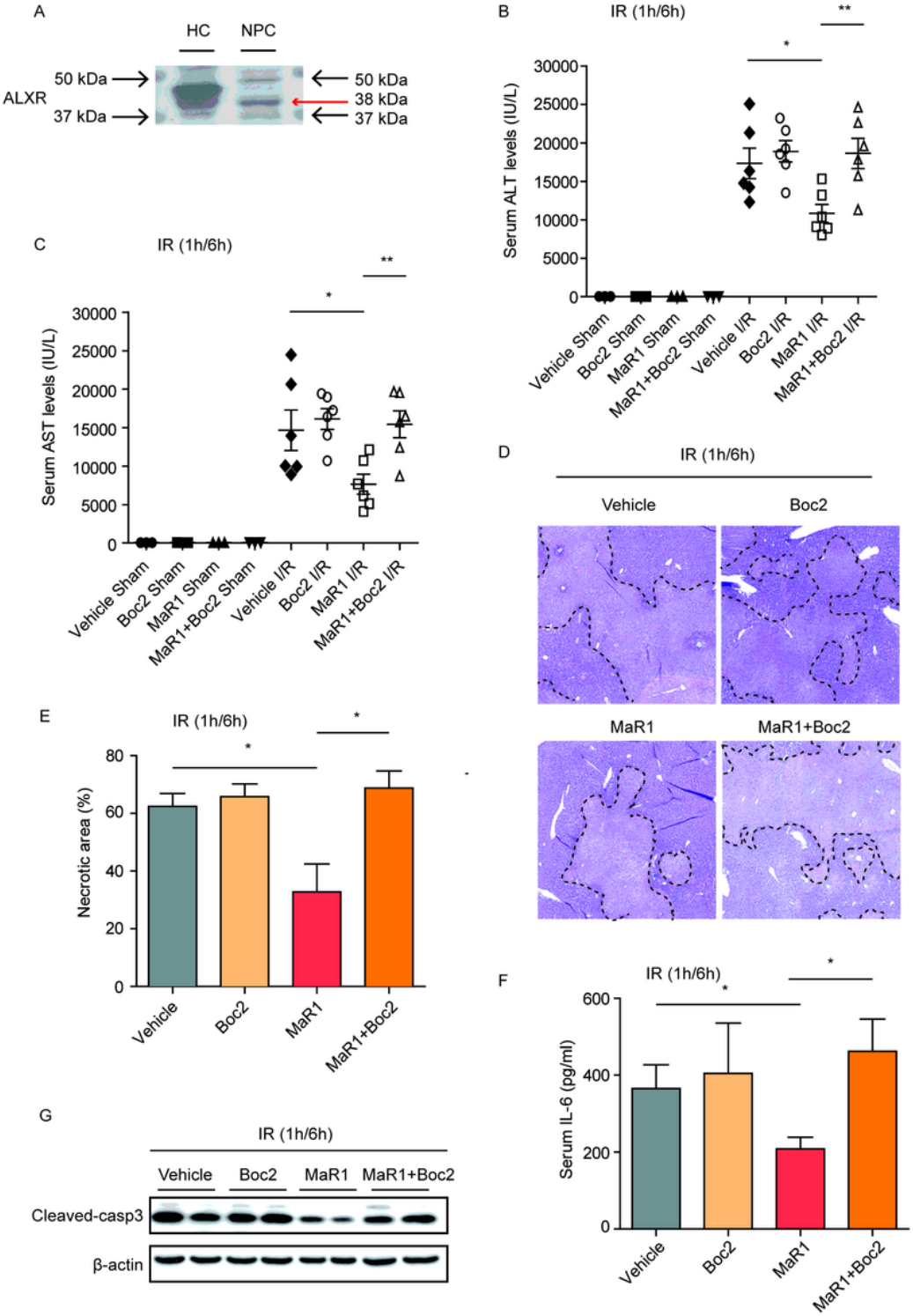

Figure 5

Inhibition of lipoxin A4 receptor (ALXR) abolishes the beneficial effects of MaR1 in I/R-induced liver damage. (A) Western blot of whole-cell lysates from primary mouse HC and NPC assessing protein expression of ALXR at the baseline. WT mice were treated with/without ALXR inhibitor (Boc2; 50mg/kg, i.p.) 1h prior to liver I/R with PBS or MaR1 (20ng/mouse, i.v.) (B, C) Serum ALT and AST levels in indicated groups after 6h reperfusion (n=3 in sham groups; n=6 in I/R groups). (D) Representative liver H&E staining (original magnification ×20) from indicated groups. (E) Quantitation of liver necrotic areas, quantified in bar graph; n = 5 for each I/R group; (F) Serum IL-6 levels in indicated groups. (G) Western blot analysis of cleaved-caspase 3 in liver tissue from mice subjected to I/R insult in the indicated group. Data are presented as mean ± SEM. *P <0.05, **P<0.01.

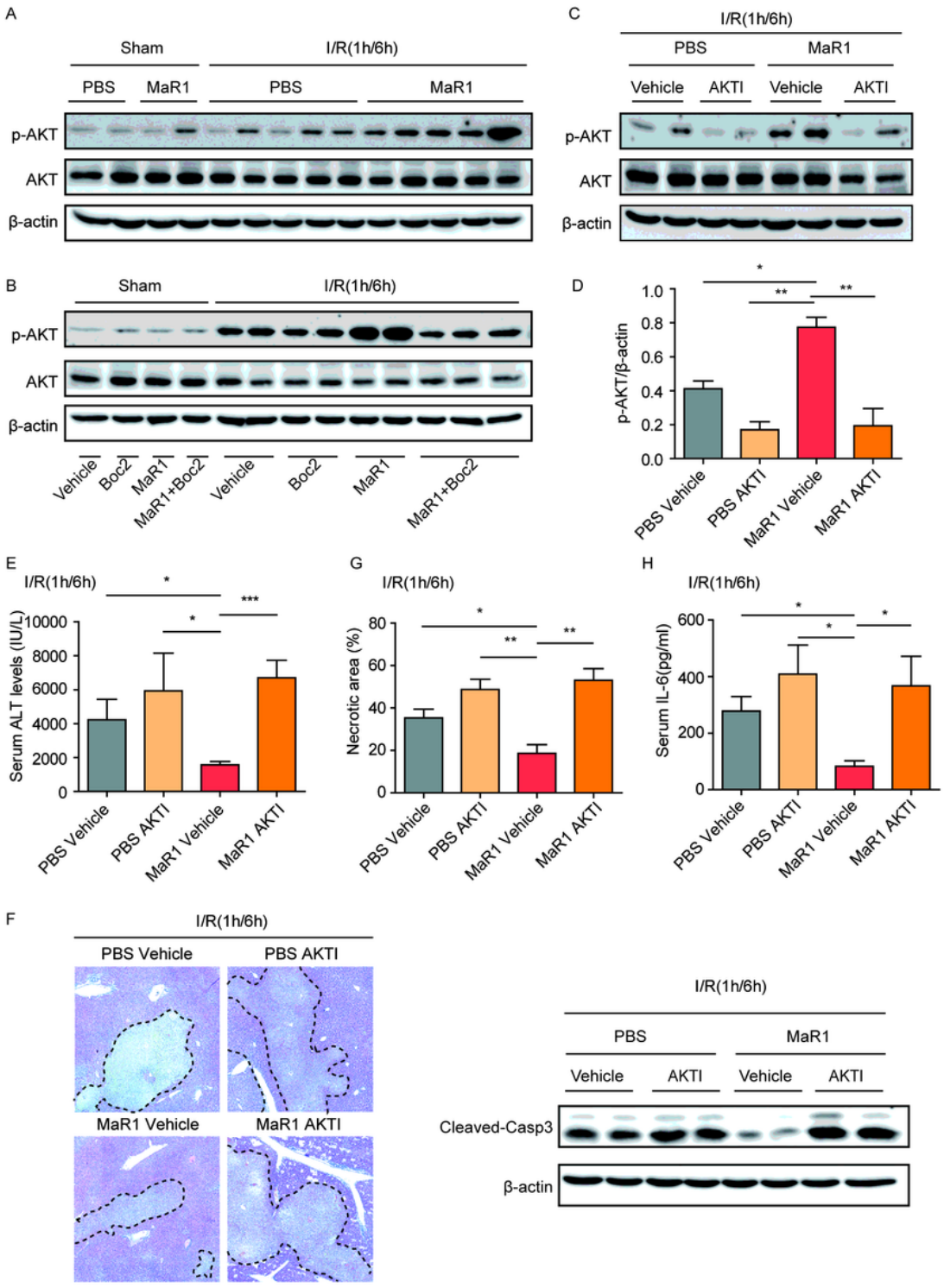

Figure 6

MaR1-induced Akt activation in hepatic I/R injury is dependent on ALXR. (A) Akt and p-Akt protein levels in mice with the treatment of PBS or MaR1 6 h after reperfusion. (B) The expression of Akt and p-Akt was evaluated by Western blot in the liver of the indicated group. (C) Western blot showing the protein levels of total and phosphorylated Akt in mice subjected to vehicle or Akt inhibitor administration with or without the treatment of MaR1. (D) Representative Western blotting and quantitative analyses revealing

p-Akt protein expression in the liver of indicated groups. (E) Serum ALT levels were measured in WT mice treated with vehicle or Akt inhibitor in the presence or absence of MaR1and harvested 6h after I/R (n =5-6 for I/R group). (F) Representative H&E images (original magnification ×20) of liver sections from WT mice treated with vehicle or Akt inhibitor in the presence or absence of MaR1and harvested 6h post-reperfusion. (G) Percentages of necrotic areas are shown in the indicated I/R groups (n=3). (H) Serum IL-6 levels of PBS- and MaR1-treated mice subjected to the vehicle or Akt inhibitor and harvested 6 h post-reperfusion as analyzed by ELISA (n=5-6 for each group). (I) Cleaved-caspase 3 protein expression of PBS- and MaR1-treated mice subjected to the vehicle or Akt inhibitor and liver tissues harvested 6 h after I/R as analyzed by Western blotting. Data are presented as means± SEM. *P <0.05, **P<0.01, ***P<0.001.

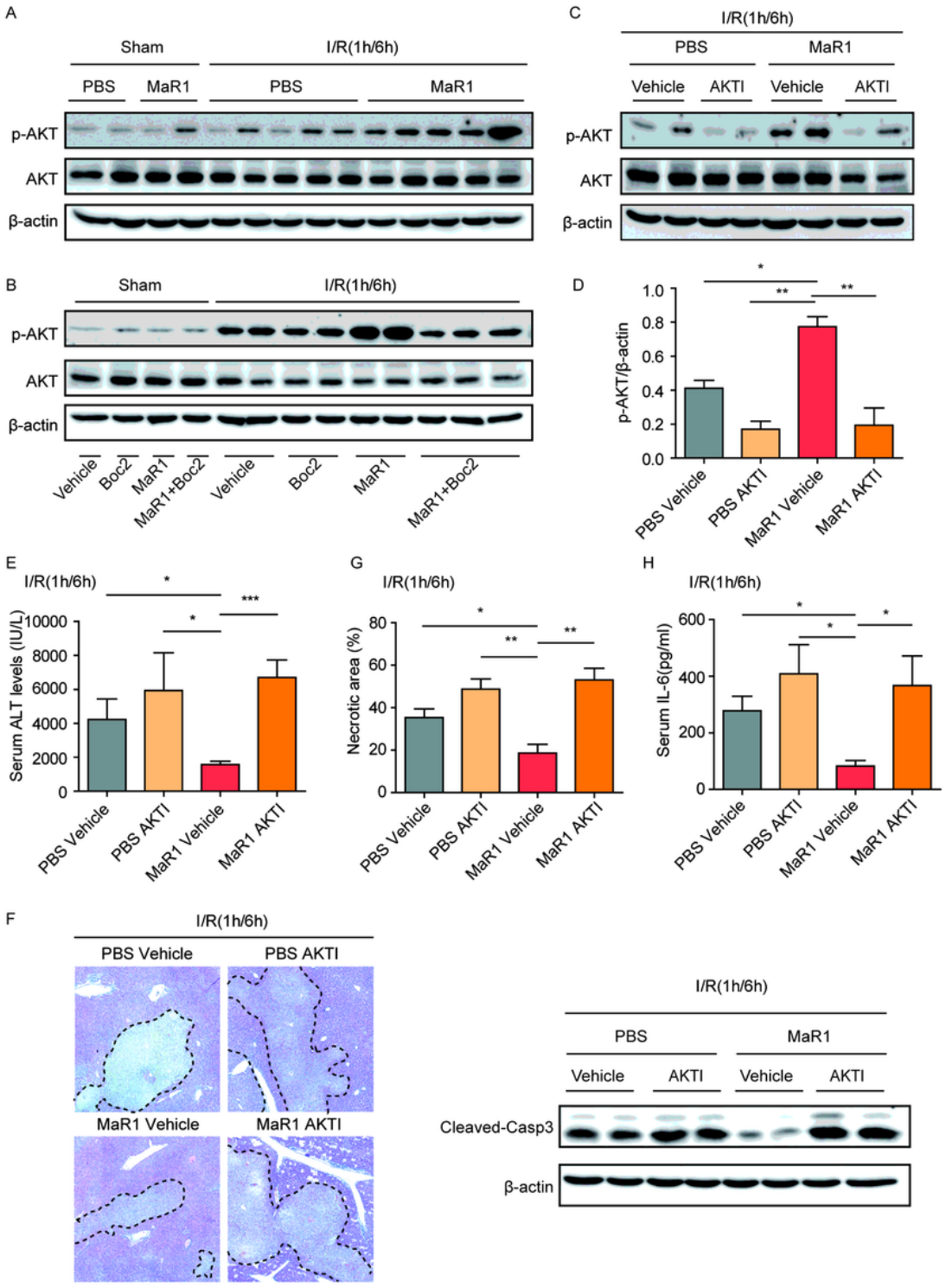

Figure 6

MaR1-induced Akt activation in hepatic I/R injury is dependent on ALXR. (A) Akt and p-Akt protein levels in mice with the treatment of PBS or MaR1 6 h after reperfusion. (B) The expression of Akt and p-Akt was evaluated by Western blot in the liver of the indicated group. (C) Western blot showing the protein levels of total and phosphorylated Akt in mice subjected to vehicle or Akt inhibitor administration with or without the treatment of MaR1. (D) Representative Western blotting and quantitative analyses revealing

p-Akt protein expression in the liver of indicated groups. (E) Serum ALT levels were measured in WT mice treated with vehicle or Akt inhibitor in the presence or absence of MaR1and harvested 6h after I/R (n =5-6 for I/R group). (F) Representative H&E images (original magnification ×20) of liver sections from WT mice treated with vehicle or Akt inhibitor in the presence or absence of MaR1and harvested 6h post-reperfusion. (G) Percentages of necrotic areas are shown in the indicated I/R groups (n=3). (H) Serum IL-6 levels of PBS- and MaR1-treated mice subjected to the vehicle or Akt inhibitor and harvested 6 h post-reperfusion as analyzed by ELISA (n=5-6 for each group). (I) Cleaved-caspase 3 protein expression of PBS- and MaR1-treated mice subjected to the vehicle or Akt inhibitor and liver tissues harvested 6 h after I/R as analyzed by Western blotting. Data are presented as means± SEM. *P <0.05, **P<0.01, ***P<0.001.

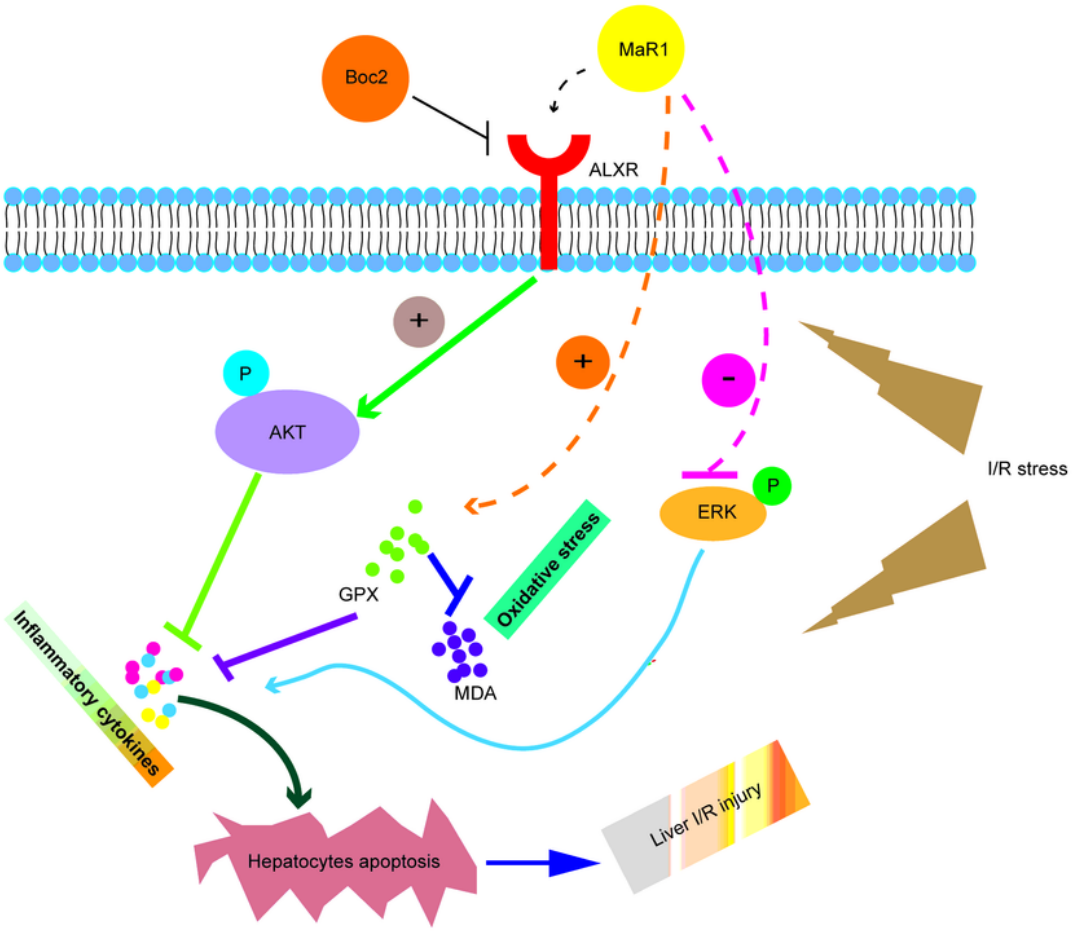

Figure 7

Proposed hepatoprotective signaling mechanisms mediated by MaR1 in liver I/R injury. MaR1 confers protection against I/R-induced liver damage through interacting with ALXR, thus resulting in enhancing downstream p-Akt protein expression. MaR1 also exerts its protective role during hepatic I/R injury by increasing antioxidant enzyme activity (GPX), inhibiting the activation of ERK and suppressing inflammatory responses, and finally contributes to decreased apoptotic cell death.

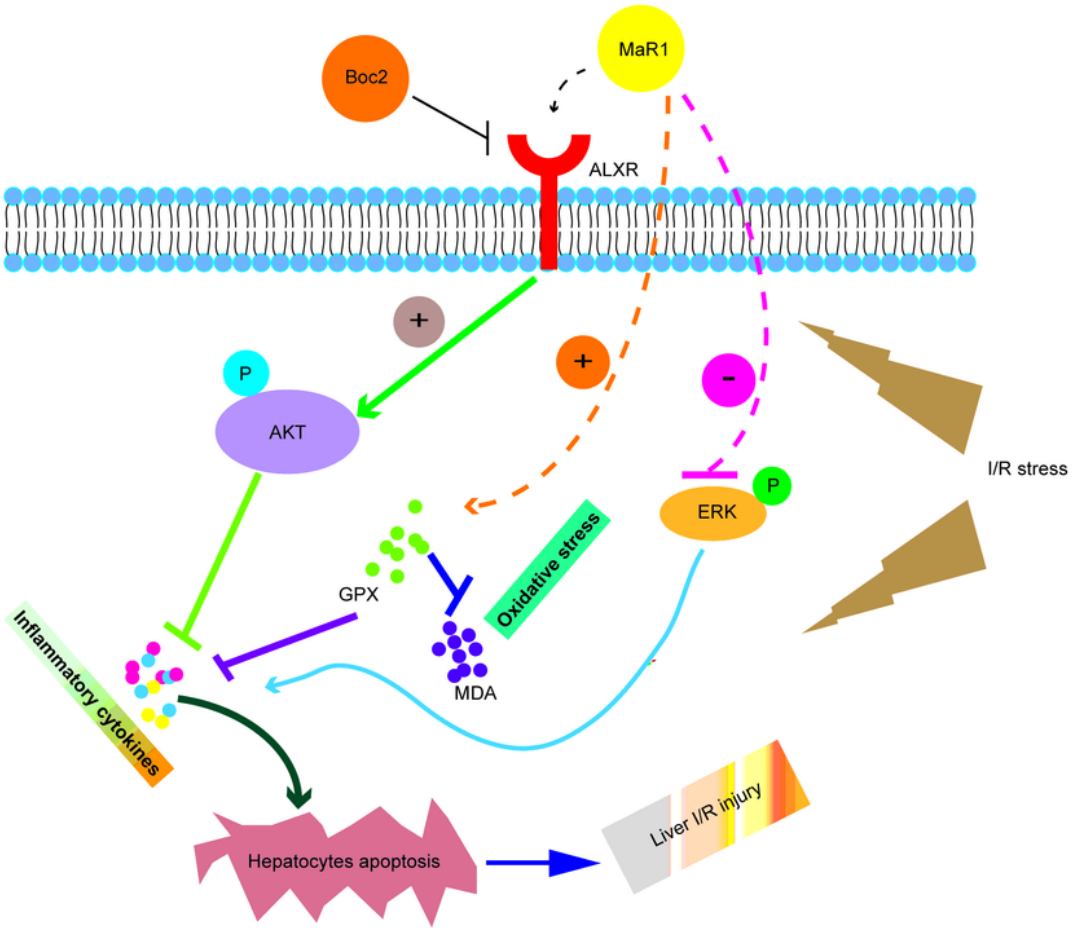

Figure 7

Proposed hepatoprotective signaling mechanisms mediated by MaR1 in liver I/R injury. MaR1 confers protection against I/R-induced liver damage through interacting with ALXR, thus resulting in enhancing downstream p-Akt protein expression. MaR1 also exerts its protective role during hepatic I/R injury by increasing antioxidant enzyme activity (GPX), inhibiting the activation of ERK and suppressing inflammatory responses, and finally contributes to decreased apoptotic cell death.

Supplementary Files

This is a list of supplementary files associated with this preprint. Click to download.

- supplementaryFig1.docx
- supplementaryFig1.docx